Ocean Engineering 213 (2020) 107681

Contents lists available at ScienceDirect

Ocean Engineering

journal homepage: www.elsevier.com/locate/oceaneng

The input vector space optimization for LSTM deep learning model in real-time prediction of ship motions

Yucheng Liu, Wenyang Duan, Limin Huang *, Shiliang Duan, Xuewen Ma

College of Shipbuilding Engineering, Harbin Engineering University, Harbin, 150001, China

ARTICLE INFO

Keywords:
Ship motions real-time prediction
LSTM deep learning model
Input vector space optimization
Impulse response function
Auto-correlation function

ABSTRACT

Vessel motions due to the ocean waves contribute to maritime operational safety and efficiency. Real-time prediction of deterministic ship motions in the coming future seconds is essential in decision-making when performing motions sensitive activities. The Long-Short Term Memory (LSTM) deep learning model provides a potential way for nonlinear ship motions prediction due to its capability in nonlinearity processing. Determination of a reasonable dimension of the input vector is critical in training the LSTM model. Conventionally, the optimal dimension for the input vector is selected by traversing an empirical preset range. Hence, it suffers both high computational cost and poor adaptation in determining the optimal input vector dimension. In the present work, an input vector space optimization method is proposed based on the dependence hidden in ship motion records of a sequence. Taking different correlation expressions into consideration, both the Impulse Response Function (IRF) based and Auto-correlation Function (ACF) based techniques are investigated for input vector space optimization. Numerical simulations are carried out for vilification and comparison purpose. The ACF technique is better in representing the auto-correlation hidden in the stochastic ship motions. And the ACF-based LSTM model performs better in both training efficiency and prediction accuracy.

1. Introduction

Real-time prediction of the deterministic vessel motions in the coming future seconds are critical in decision-making for performing motion sensitive maritime activities. Therefore, it is extensively studied in various subjects such as ship-borne helicopter recovery (Yang, 2013), ship motions active stabilization (Huang et al., 2018), and fire control (Huang et al., 2014). A variety of models have been attempted to achieve real-time prediction of vessel motions. These models are classified into three types, the linear hydrodynamic equations based prediction model, classic time series prediction models and the machine learning based prediction models.

Early studies on the real-time ship motions prediction were developed based on the linear ship hydrodynamic equations. The linear hydrodynamic equations based prediction models, for example, convolution method based on ship response kernel function (Kaplan, 1965) and state-space approaches based on Kalman filtering techniques (Triantafyllou et al., 1981, 1982, 1983) depend on the accuracy ship hydrodynamic coefficients solved in frequency domain. However, the ship hydrodynamic coefficients are time-varying in high sea states and are difficult to obtained in the stochastic sea conditions due to the unknown simulation boundaries. Therefore, their performances are far from expected.

Improvements on real-time prediction of ship motions were obtained by using time series analysis. Time series prediction models are data-driven. Only the ship motions records are required when modeling. The auto-regressive (AR) model is one of the most explored (Huang et al., 2014) due to its simplicity and practicability. To further improve the prediction accuracy, the auto-regressive moving average (ARMA) model is developed (Yumori, 1981) by using the coming wave records as inputs in addition to the ship motions samples. The classic time series models are generally developed based on linear and stationary theories and hence suffer difficulties in nonlinear and non-stationary ship motions modeling. In addition, Nielsen et al. (2018) proposes a method of ship motion prediction based on auto-correlation function, without fitting parameters, prediction can be made entirely using the ACF and a short period (10–30 s) of the back-dated time series, this method achieved good results under different sea conditions.

In recent years, machine learning based prediction models were developed to real-time prediction of nonlinear ship motions due to their

* Corresponding author.
E-mail address: huanglimin@hrbeu.edu.cn (L. Huang).

https://doi.org/10.1016/j.oceaneng.2020.107681
Received 22 January 2020; Received in revised form 18 June 2020; Accepted 20 June 2020
Available online 4 August 2020

capability in nonlinearity processing. Which include neural network method (Wang et al., 1997), fuzzy mathematics method (Khan et al., 2007), and chaos theory method (WENG et al., 2010) etc. Thanks to the improvements in computer engineering, the deep learning techniques were extensively investigated in time series modeling. The recurrent neural networks (RNN), a kind of deep learning techniques, is suitable for time series processing. It was extensively explored in stock market prediction (Akita et al., 2016), literal translation (Graves et al., 2009), traffic flow forecasting (Shao et al., 2016; Chen et al., 2016; Zhao et al., 2017), wind speed forecasting (Liu et al., 2018), etc. However, the original RNN model suffers gradient explosion and vanish. These difficulties are overcome by adding saving and forgetting mechanisms in the neural networks (Hochreiter et al., 1997; Gers et al., 1999). This kind of model is designated as long short-term memory (LSTM) neural networks. The LSTM model was employed in ship motions time series modeling problems such as deterministic ship motions estimation with wave-excitations (Duan et al., 2019) and estimating relative wave direction from in-service ship motion measurements (Mak et al., 2019).

Determination of a reasonable dimension of the input vector is critical in training the LSTM model. Too small dimension of the input vector leads to under-fitting as the relations between the inputs and outputs are not well modeled. In contrast, too large dimension of the input vector results in over-fitting and higher computational cost. The determination of input vector dimension is similar to the order selection in classic time series models identification. The training residuals with respects to model orders in a preset range need to be calculated. Then the optimal order is selected by applying the information criteria such as AIC (Akaike, 1974) and BIC (Akaike, 1979) principles on the training residuals. It suffers both high computational cost and poor adaptation in determining the optimal model order (Duan et al., 2015). Inspired by the memory effects hidden in the ship motions time series, *Duan* et al. (2015) addressed an impulsive response function (IRF) based order selection technique for the AR model identification. Both computational efficiency and robustness were obviously improved.

The optimal input vector space selection, or determine the number of past time samples included for predicting ahead of time for the LSTM model faces the same difficulties as the conventional time series models order determination. Therefore, we hope to find an efficient, highly adaptive and more accurate method to determine the input vector space of the LSTM model used for the prediction of the ship motion time series, or estimate the optimum number of samples to be included. In the present work, an input vector space optimization method is proposed based on the dependence hidden in ship motion records of a sequence. By taking different correlation expressions into consideration, both the Impulse Response Function (IRF) based and Auto-correlation Function (ACF) based techniques are investigated for input vector space optimization. Numerical simulations are carried out for verification and comparison purpose.

The rest of the paper is organized as follows. Section 2 presents the methodology for LSTM deep learning network. Formulations for the proposed auto-correlation based input vector space optimization techniques are given in section 3. In section 4, results and discussion are presented, the effect of the ACF function in input vector space optimization is analyzed. Finally, section 5 summarizes the concluding remarks of the present research work.

2. Methodology for LSTM deep learning network

The RNN model is a deep learning technique designed to solve time sequence modeling problems. It is capable of solving nonlinear time series problems. When training the RNN model, we will expand the recurrent layer in the model into a fully connected layer with the same weight. The number of steps in the input feature needs to be the same as the number of layers in the recurrent layer. We call it the characteristic memory length, or the length of the feature input on the time axis. When the memory length is too long, the training efficiency of the model will decrease. At the same time, vanish gradient and exploding gradient will inevitably occur during the training process. This means that the RNN model cannot handle the problem when those input features have a long memory length. In order to meet the needs of practical problems, some researchers have created Long-Short-Term Memory network models (LSTM). LSTM neuron structure is based on the self-recurrent structure of the RNN model. Different from the traditional RNN model, the LSTM model constructs a stable state stream during data self-looping, and control the state of neurons at each moment through an update structure with input gate, forget gate, and output gate. Neurons remember the input of the previous moment through the state of the cell. The existence of the update structure transforms the relationship between the output of the current moment and the output of the previous moment from a composite function to a linear superposition of multiple independent functions. This can reduce the possibility of vanish gradient or exploding gradient in the process of solving the gradient.

For a time series $x = (x_1, x_2, ..., x_n)$, Traditional RNN neurons (as shown in Fig. 1) calculate a state sequence $h = (h_1, h_2, ..., h_n)$ and an output sequencey $= (y_1, y_2, ..., y_n)$. Their calculation process can be expressed as:

$$h_n = f(W_{xh}x_n + W_{hh}h_{n-1} + b_h) \tag{1}$$

$$y = \phi(W_{hy}h + b_y) \tag{2}$$

In the formula, W represents the weight matrix, b represents the offset vector, and f represents the activation function.

The LSTM model replaces the RNN neurons in hidden layer with LSTM neurons, which will empower the model for long-term memory. The most widely used LSTM model structure is shown in Fig. 2.

In this structure, i, f, o, c represent the input gate, the forgetting gate, the output gate and the cell state respectively, where tanh is the hyperbolic tangent activation function. The input gate, the forgetting gate, and the output gate are shown as equation (3)-(5):

$$i_n = \sigma(W_{xi}x_n + W_{hi}h_{n-1} + b_i) \tag{3}$$

$$f_n = \sigma(W_{xf}x_n + W_{hf}h_{n-1} + b_f) \tag{4}$$

$$o_n = \sigma(W_{xo}x_n + W_{ho}h_{n-1} + b_o) \tag{5}$$

For LSTM neuron status c, it is shown in equation (6)

$$c_n = f_n c_{n-1} + i_n \tanh(W_{xc}x_n + W_{hc}h_{n-1} + b_c) \tag{6}$$

For LSTM neuron hidden state h, it is shown in equation (7):

$$h_n = o_n \tanh(c_n) \tag{7}$$

W is the weight coefficient matrix, b is the offset vector, σ is the activation function. Correspondingly, c_n and h_n respectively represent the cell state and hidden state of the LSTM structure in the nth time step. Among them, the maximum n will not exceed our preset input vector space of feature.

An RNN neural network is usually composed of several RNN layers and the last fully connected layer, the LSTM network will use the LSTM

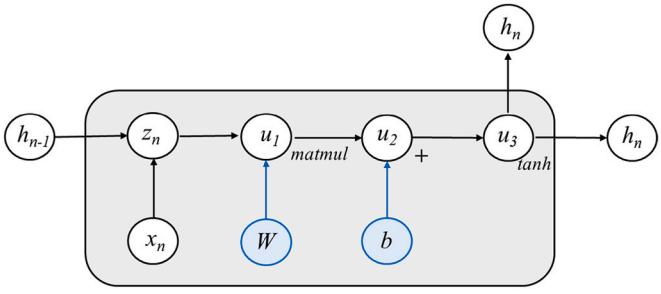

Fig. 1. Standard RNN structure.

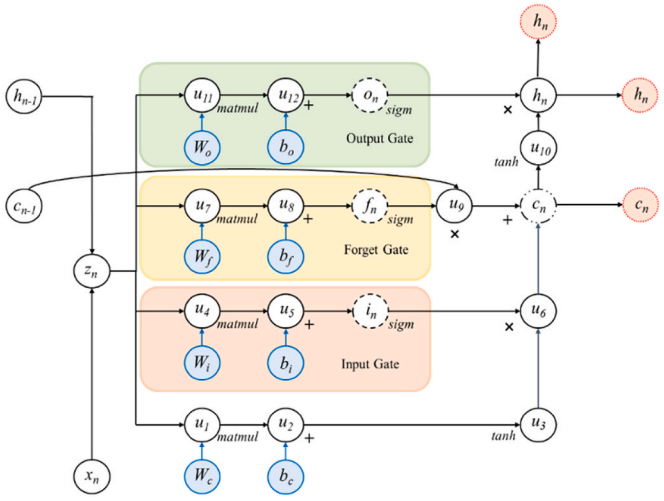

Fig. 2. LSTM structure.

layer to replace the RNN layer. After the LSTM structure completes the sequence feature extraction, these features will be input into a fully connected layer for processing to obtain the final output of the entire neural network, as shown in equation (8):

$$y = \phi\left(W_{hy}h + b_y\right) \tag{8}$$

y is a vector, and its dimension is determined when designing the network. When the LSTM model is applied to ship motion prediction, it represents all predicted future ship motion.

Like all neural network models, the initialization neurons parameters of the LSTM neural network and RNN neural network are randomly generated. It uses the data of the training set to calculate the loss function, and based on the BPTT algorithm (Boden, 2002) to reverse solve the gradient, and then adjust the model neurons parameters according to the gradient until convergence. Gers et al. (1999) pointed out that the existence of the forget gate structure avoids the vanishing gradient caused by the continuous product in the process of solving the weight matrix gradient in the LSTM model.

3. Auto-correlation based input vector space optimization techniques

3.1. The impulsive response function

Different with time series of traffic flow and stock price etc., ship motions time series have obvious memory effects. The memory effects are consequences of the radiated waves result from the ship motions and their scattering of incident waves. This means the waves generated by the ship motions will persist and affect subsequent ship motions. That is the present ship motion is related to the past ship motion records. Under the linear theoretical assumptions, the memory effects of ship motions can be reasonably modeled by using the impulsive response function (IRF) (Cummins, 1962; Liapis, 1986). The magnitudes of the IRF represent the effects of the past ship motions on the present ship motions.

In order to model the ship motions memory effects, the ship is regarded as a linear system. The ship motions are inputs while the hydrodynamic forces on the ship induced by the motions are outputs. The ship motions equations using the IRF are described as the following forms (Cummins, 1962; Liapis, 1986).

$$\sum_{j=1}^{6}\left\{\left(M_{jk}+m_{jk}\right)\ddot{\eta}_j + \int_0^t h_{jk}(t-\tau)\dot{\eta}_j(\tau)d\tau + d_{jk}\eta_j\right\} = F_k(t) \quad \left(k=1,\ldots,6\right) \tag{9}$$

where $\boldsymbol{M}_{jk}$ and $\boldsymbol{m}_{jk}$ are the inertial mass matrix and added mass matrix of the ship. $F_k(t)$ are time-varying generalized external forces including the incident wave force, diffraction force, etc. $h_{jk}(\tau)$ are IRFs that represents the memory effects of ship motion. The indices jk represents the contribution of the j-th mode impulsive velocity of ship motion in IRF respect to the k-th mode. The t and τ represent the current time and the length of time back from the current time.

Under the assumption that each degree of freedom of motion is independent, the equation for ship motion with memory effects in one degree of freedom can be modeled using a generalized form as shown in Eq. (10).

$$(\mathrm{M}+m)\ddot{\eta}(t) + \int_{-\infty}^{t} h(\tau)\dot{\eta}(t-\tau)d\tau + D\eta(t) = F(t) \tag{10}$$

where$\eta(t)$, $\dot{\eta}(t)$and$\ddot{\eta}(t)$ represent the ship motion displacement, velocity and acceleration, respectively. The inertial mass and added mass are respectively designated as M and m. $F(t)$ is the external force acting on the ship while D is the hydrostatic restoring coefficient. $h(\tau)$ is IRF that related to the degree of freedom motion$\eta(t)$.

Firstly, we defines a differential operators

$$\Delta\eta = \eta_n - \eta_{n-1} \tag{11}$$

Subsequently, the ship motion equation in (10) can be discretized into finite terms. Eq. (10) is reformulated as

$$\frac{\Delta^2\eta_n}{(\Delta t)^2} + h_1\frac{\Delta\eta_n}{\Delta t} + h_2\frac{\Delta\eta_{n-1}}{\Delta t} + \ldots + h_l\frac{\Delta\eta_{n-l+1}}{\Delta t} + D\eta = F_n \tag{12}$$

$$\frac{1}{(\Delta t)^2}(\eta_n - 2\eta_{n-1} + \eta_{n-2}) + \frac{h_1}{\Delta t}(\eta_n - \eta_{n-1}) + \ldots + \frac{h_l}{\Delta t}(\eta_{n-l+1} - \eta_{n-l}) + D\eta_n = F_n \tag{13}$$

Collecting the terms, equation (13) becomes

$$\left\{1 + h_1\Delta t + D(\Delta t)^2\right\}\eta_n + (h_2\Delta t - h_1\Delta t - 2)\eta_{n-1} + \ldots + (h_l\Delta t - h_{l-1}\Delta t)\eta_{n-l+1} + (-h_l\Delta t)\Delta\eta_{n-l} = F_n(\Delta t)^2 \tag{14}$$

Let

$$\phi_1 = 1 + h_1\Delta t + C(\Delta t)^2; \phi_2 = \mathrm{h}_2\Delta t - h_1\Delta t - 2; \phi_3 = 1 + h_3\Delta t - h_2\Delta t;$$
$$\phi_4 = \mathrm{h}_4\Delta t - h_3\Delta t; \ldots\phi_l = \mathrm{h}_l\Delta t - h_{l-1}\Delta t; \phi_{l+1} = -h_l\Delta t; \tag{15}$$

Replacing the terms of equation (15) using simple forms in equation (14), we can obtain

$$\phi_1\eta_n + \phi_2\eta_{n-1} + \phi_3\eta_{n-2} + \ldots + \phi_l\eta_{n-l+1} + \phi_{l+1}\eta_{n-l} = F_n \tag{16}$$

As shown in (16), it is suggested that the ship motion in ocean wave is an AR process. It may be modeled using AR model with an order of p, designated as $AR(p)$. Discrete process of the ship motion equation as shown in (15) indicates that the model order p to model the ship model depends on the convolution of $\int_0^\infty h(\tau)\dot{x}(t-\tau)d\tau$.

Ship impulse response function can be calculated in the time or frequency domain. Since it is difficult to solve the impulse response function in the time domain, we use the Kramers-Konig relations to solve it in the frequency domain. As shown in (17):

$$h_{jk}(\tau) = \frac{2}{\pi}\int_0^\infty\left\{\omega_e m_{jk} - \omega_e A_{jk}(\omega_e) - \frac{1}{\omega_e}d_{jk}\right\}\sin\omega_e\tau d\omega_e \tag{17}$$

ω_e is the encounter frequency.

Example in Fig. 3 presents the IRF of heave, from which it is found that the strength of memory effect $h(\tau)$ decreases as time variable τ increases and is close to zero. Among them, t and τ represent the current time and the length of time back from the current time.

Obviously, the value of the ship motion impulse response function tends to 0 gradually as the distance increases. And the value of the

impulse response function is related to the added mass coefficients, damping coefficients, hydrodynamic restoring coefficient and encounter frequency. Therefore, the ship impulse response function of known ship type and working condition can be calculated by hydrodynamic method. According to the impulse response function curve, it is close to zero infinitely when τ exceeds the threshold value τ_0, if the sampling interval of the ship's motion time series is Δt, then we can get the time-length of the model input p, which is:

$$p = \frac{\tau_0}{\Delta t} \tag{18}$$

3.2. The auto-correlation function

Correlation coefficient is an important concept in time series analysis. We use auto-covariance $K_x(\tau) = E[X(t)X(t+\tau)]$ to quantify the degree of correlation between values at different times in a time series. But the value of the auto-covariance is related to the value of the two points that are related to each other. Therefore, we need to use the dimensionless auto-covariance to represent the correlation of time series. As shown in Formula (19):

$$r_x(\tau) = \frac{K_x(\tau)}{K_x(0)} = \frac{R(x) - m_x^2}{\sigma_x^2} \tag{19}$$

We call $r_x(\tau)$ the auto-correlation function (ACF) of time series X(t), and use it to represent the degree of correlation between any two points with the same time interval. There may be a positive or negative correlation between the two points, in which the smaller the absolute value of the value of X, the weaker the correlation between the two points. Nielsen et al. (2018) point out that using directly the time series to calculate the autocorrelation function may cause the ACF curve fails to damp out according to expectation. Considering that the ship motion prediction model usually based on the time series method requires an input time series length not exceeding 50 s, the slight oscillation of the ACF curve (not more than 0.25) at this length of time will not affect its accuracy in determining the input vector space. In addition, Nielsen et al. (2018) proposed a method of using the response spectrum to calculate the auto-correlation function. This is an interesting idea and seems to be able to better guarantee the convergence of the ACF curve.

Generally, as τ grows, the absolute value of $r_x(\tau)$ tends to decrease which means that the degree of correlation between the two is weakening. When the absolute value of $r_x(\tau)$ is small enough, we can believe that there is no correlation between the two points. Therefore, there is a τ_0 and r, so for any $\tau > \tau_0$, there is always $r_x(\tau) < r_x(\tau_0)$. We call τ_0 the related time of the time series.

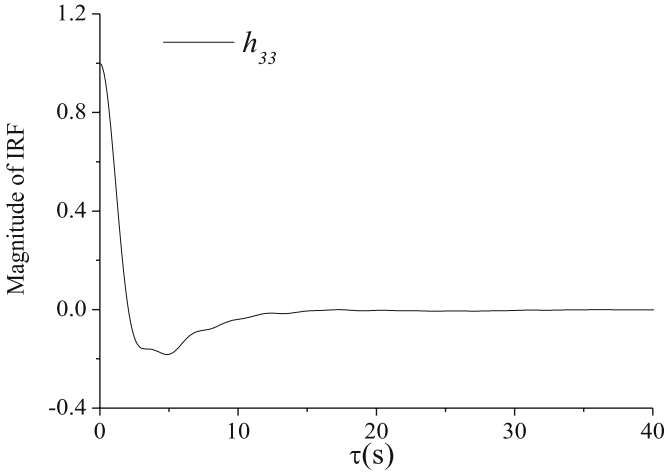

Fig. 3. Ship heave motion impulse response function.

4. Results and discussion

4.1. Brief descriptions of the nonlinear ship motions

In this paper, we use the numerical simulation motion data of the S175 container ship. The corresponding sea conditions are the sea state 4 and the sea state 5. In order to reflect the non-linearity of the actual sea condition, the GN numerical model is used to generate the wave duration. Based on the generated wave duration, nonlinear time domain simulation method can be used to generate ship motion data.

The equations of motion for ship heave and pitch can be expressed as follows:

$$(M+\mu_{33})\ddot{\eta}_3 + b_{33}\dot{\eta}_3 + \int_0^t K_{33}(t-\tau)\dot{\eta}_3 d\tau + c_{33}\eta_3 + \mu_{35}\ddot{\eta}_5 + b_{35}\dot{\eta}_5 + \int_0^t K_{35}(t-\tau)\dot{\eta}_5 d\tau + c_{35}\eta_5 = F_3^{IS} + F_3^D + F_3^{slamming} - Mg \tag{20}$$

$$(I_{yy}+\mu_{55})\ddot{\eta}_5 + b_{55}\dot{\eta}_5 + \int_0^t K_{55}(t-\tau)\dot{\eta}_5 d\tau + c_{55}\eta_5 + \mu_{53}\ddot{\eta}_3 + b_{53}\dot{\eta}_3 + \int_0^t K_{53}(t-\tau)\dot{\eta}_3 d\tau + c_{53}\eta_3 = F_5^{IS} + F_5^D + F_5^{Slamming} \tag{21}$$

In the above equation of, M is the ship mass, I_{yy} represents the pitching moment coefficient of inertia of the ship over the center of gravity. $\mu_{33}, \mu_{55}, \mu_{35}, \mu_{53}$ are the high frequency additional mass coefficient for the heave and pitch of ship motion. $b_{33}, b_{55}, b_{35}, b_{53}$ are the high frequency damping coefficient for ship motions. c_{33}, c_{35}, c_{53}, c_{55} are the coefficient of restoring force in the direction of heave and pitch of ship motions. $k_{33}, k_{55}, k_{35}, k_{53}$ are the impulse response functions of radiation force in the direction of heave and pitch of ship motions. The F^{IS} on the right side of the equation represents the resultant forces of incident wave force and hydrostatic recovery force. $F^D$and $F^{slamming}$are diffraction force and slamming force.

When the incident wave and hydrostatic pressure P_{IS} are integrated on the instantaneous wet surface of the ship, the non-linear incident wave force and hydrostatic recovery force can be expressed as follow:

$$\mathbf{F} = \iint_{S(t)} P_{IS}\vec{n}\,ds \tag{22}$$

$$M = \iint_{S(t)} P_{IS}\left(\vec{r}_g \times \vec{n}\right) ds \tag{23}$$

For the non-linear incident wave force and hydrostatic restoring force, the incident wave and hydrostatic pressure in integral formula is the basis of the whole accurate calculation process.

According to the derivation of Zhao et al. (2015), the pressure at any point in the GN wave model can be written as follow:

$$p = \rho\left[g(\beta - z) - \sum_{n=0}^{K}\frac{\partial w_n}{\partial t}T1_n + \sum_{n=0}^{K}\sum_{m=0}^{K}u^m\frac{\partial w_n}{\partial x}T2_{nm} + \sum_{n=0}^{K} \times \sum_{m=0}^{K} w^m \cdot w^n \cdot T4_{nm}\right] \tag{24}$$

$$T1_n = \int_z^{\beta}\left(e^{az}\cdot z^n\right) \tag{25}$$

$$T2_{nm} = \int_z^{\beta}\left(e^{2az}\cdot z^{n+m}\right)dz \tag{26}$$

$$T4_{nm} = \int_z^{\beta} e^{2az}\left(a\cdot z^{n+m} + n\cdot z^{n+m-1}\right)dz \tag{27}$$

The total duration of motion data is 7998 s, and the sampling interval

is 0.5 s. For each set of data, we use the first 7498 s data as a train set to generate model, and use the remaining data as a test set to measure the performance of the model. Main particulars of S175 container ship are presented in Table 1. And the partial ship motion time series under different sea states are shown in Figs. 4–7.

4.2. The effects of the input vector space on the prediction accuracy

We use the LSTM model to predict the motion of the S175 container ship. Model has a hidden layer, and the number of units in the LSTM layer is 20. The optimizer used by the model is Adam (Kingma et al., 2015), and we set the activator parameter to learning-rate = 0.001, beta_1 = 0.9, beta_2 = 0.999, epsilon = 1×10^{-8}. In addition, the model sets batch size to 64 and epoch to 3000, and uses the mean square error as the loss function. Starting with a smaller value, we train a series models which feature with different sizes of the input vector space as input, until the model results show a significant deterioration trend. And we use these models to predict the heave and pitch motion of the S175 container ship after 5 s under the condition of sea state 5 and sea state 6. The root mean square error between the motion pre-diction value and the real value obtained by the model are calculated separately. The result is shown in Fig. 8 and Table 2.

The prediction error of traditional Auto-Regressive model for short-term prediction for ship motion generally decreases with the increase of the input vector space of model input features, and finally stabilizes (Akaike et al., 1979). From the results of the calculation, it is known that the LSTM model is different from the Auto-Regressive model. As the input vector space of model input features increases, the related information received by the model increases, which makes the prediction error of the model gradually decrease until a threshold. After exceeding this threshold, as the input vector space of model input features increases, the model begins to accept more and more irrelevant input information. The input of irrelevant information causes the model to try to approximate the random noise, which leads to a decrease in the generalization ability of the model and makes the prediction error of the model in the test set begin to increase.

In order to verify our conclusion, we have designed ship heave motion prediction models with different advance prediction times T_p. And compare the results of models with different input vector space of model input features. The result is shown in Fig. 9 and Table 3.

The new calculation results are in line with our conclusions. When we use the LSTM model to predict ship motion, there is a certain optimal value for the input vector space of model input features. This optimum value is related to the working conditions of the ship motion, but not related to the forecast time.

4.3. Optimized input vector space by the auto-correlation based techniques

4.3.1. The IRF based optimization technique

We calculated all the impulse response function of the S175 container ship and normalized the results. In all impulse response functions, h_{33} and h_{35} are related to the ship heave motion, and h_{53} and h_{55} are related to the ship pitch motion. As τ increases, the normalized impulse response function drops rapidly and eventually converges at 0. Considering the existence of calculation errors, we believe that when $\epsilon <$ 0.01, it can be determined that the impulse response function has converged. The maximum convergence time of the relevant impulse response function is used to determine the input vector space of model input features of the model. The result is shown in Fig. 10 and Table 4.

Table 1
Main particulars of S175 container ship.

Item	Value	Item	Value
Length between pp	175 m	Block coefficient	0.572
Beam	25.4 m	LCG relative to midship	−2.48 m
Draught	9.5 m	Long, radius gyr. Kyy/Lpp	0.24
Displacement	24742ton	Forward speed	0 knots

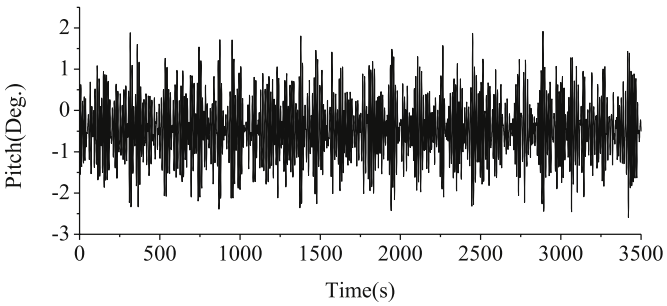

Fig. 4. Time series of pitch motion under the condition of sea state 5.

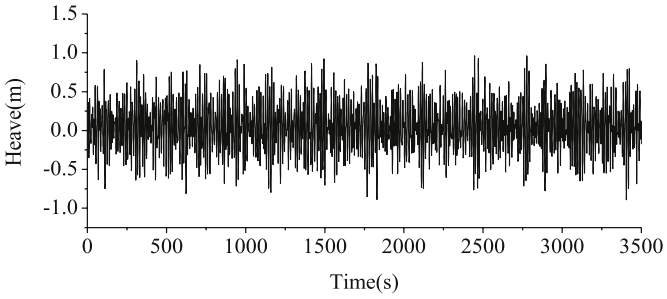

Fig. 5. Time series of heave motion under the condition of sea state 5.

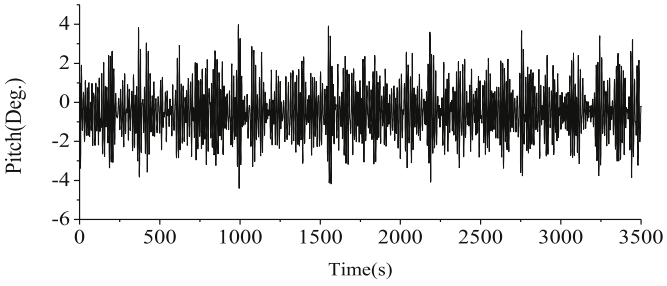

Fig. 6. Time series of pitch motion under the condition of sea state 6.

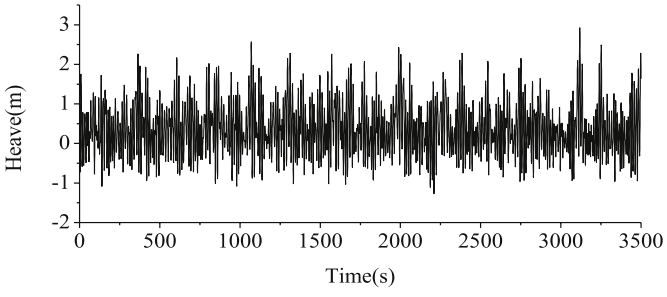

Fig. 7. Time series of heave motion under the condition of sea state 6.

4.3.2. The ACF based optimization technique

For the heave and pitch motion of the S175 container ship under the condition of sea state 5 and sea state 6, we tried to calculate ACF using data with different window length. Interestingly, when the window length is large enough (such as 3000s), the ACF curve does not change significantly with the change of the window length, and when the window length is too small, as the calculated window length changes,

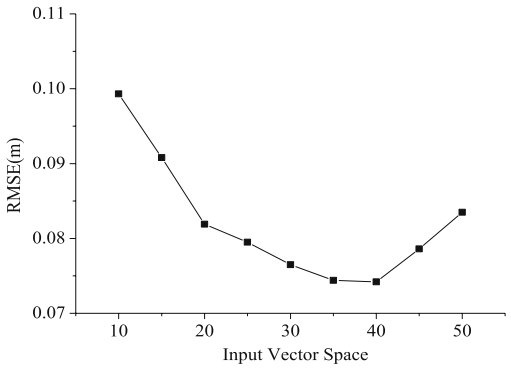

（a）RMSE of heave motion under the condition of sea state 5

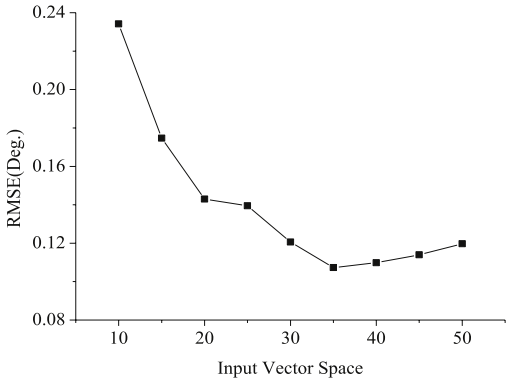

（b）RMSE of pitch motion under the condition of sea state 5

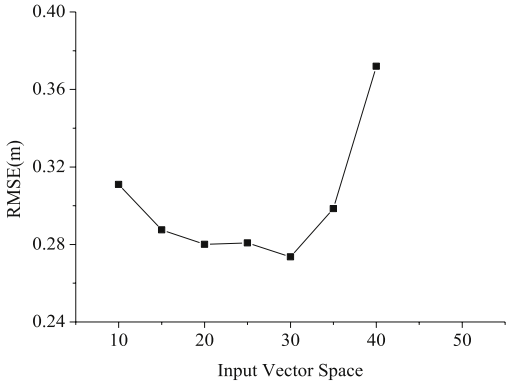

（c）RMSE of heave motion under the condition of sea state 6

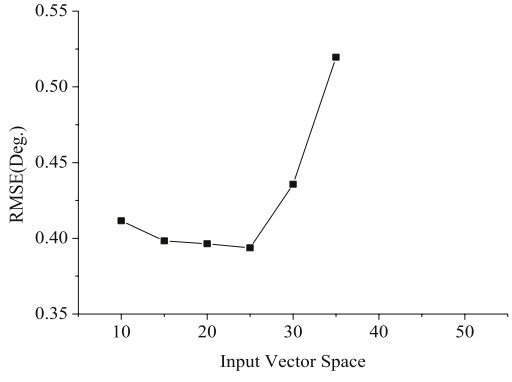

（d）RMSE of pitch motion under the condition of sea state 6

Fig. 8. The influence of input vector space of model input features on model prediction results.

Table 2
The influence of input vector space of model input features on model prediction results.

Input Vector Space	Sea state 5		Sea state 6	
	Heave motion RMSE ($\times 10^{-2}$m)	Pitch motion RMSE ($\times 10^{-1}$ °)	Heave motion RMSE ($\times 10^{-1}$ m)	Pitch motion RMSE ($\times 10^{-1}$ °)
10	9.93	2.342	3.110	4.115
15	9.08	1.747	2.875	3.983
20	8.19	1.430	2.801	3.964
25	7.95	1.395	2.808	3.937
30	7.65	1.206	2.736	4.357
35	7.44	1.073	2.985	5.196
40	7.42	1.098	3.720	–
45	7.86	1.140	–	–
50	8.35	1.197	–	–

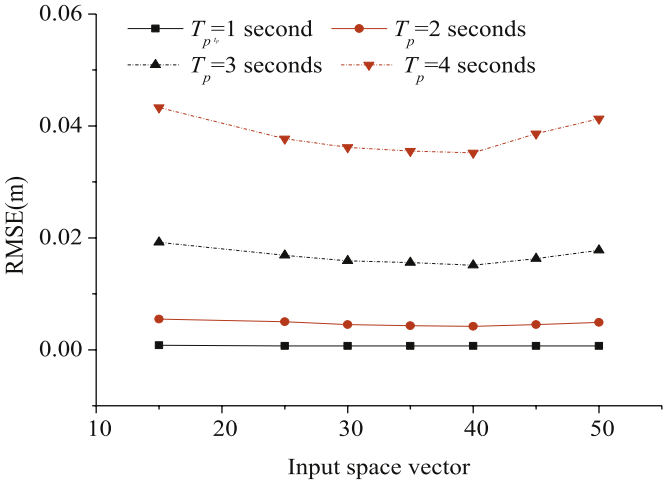

Fig. 9. The influence of input vector space of model input features on model prediction results.

Table 3
The influence of input vector space of model input features on model prediction results.

Input Vector Space	$Tp = 1$ s RMSE ($\times 10^{-4}$m)	$Tp = 2$ s RMSE ($\times 10^{-3}$ m)	$Tp = 3$ s RMSE ($\times 10^{-2}$ m)	$Tp = 4$ s RMSE ($\times 10^{-2}$ m)
15	8.0	5.5	1.92	4.33
25	7.0	5.0	1.69	3.77
30	7.0	4.5	1.59	3.62
35	7.0	4.3	1.56	3.55
40	7.0	4.2	1.51	3.52
45	7.0	4.5	1.63	3.86
50	7.0	4.9	1.78	4.13

the ACF curve will change significantly. The ACF of the heave motion of the S175 container ship under the sea state 5 calculated by different window lengths is shown in Fig. 11.

In the following content, we use all training set data (7498s) to calculate the Auto-correlation function of the motion time series and used to determine the input vector space of the model under different sea conditions. We believe that when the correlation coefficient of the time series is less than 0.5, it can be concluded that there is no enough correlation between the two. Considering the existence of calculation errors, we believe that when $r < 0.45$, it can be determined that the correlation coefficient is small enough. The minimum time that the correlation coefficient is not above this value is used to determine the input vector space of model input features of the model. The result is

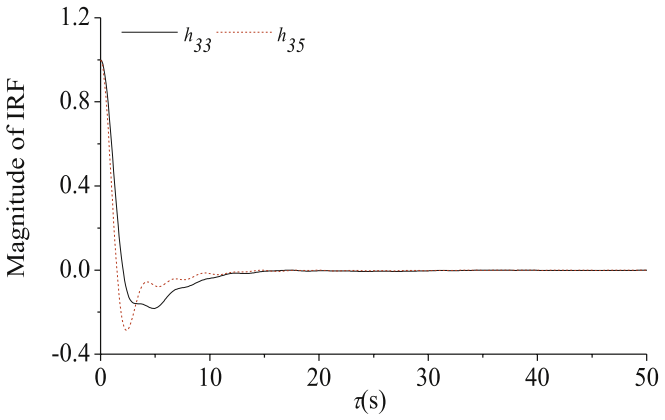

(a) Impulse response functions h_{33} and h_{35}

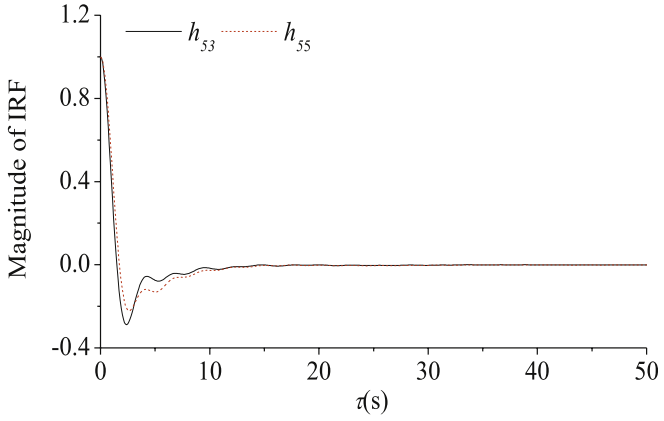

(b) Impulse response functions h_{53} and h_{55}

Fig. 10. Ship motion impulse response functions.

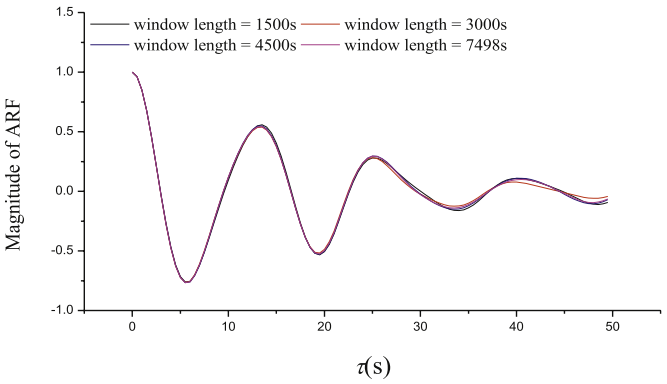

(a) ACF calculated from large enough window lengths

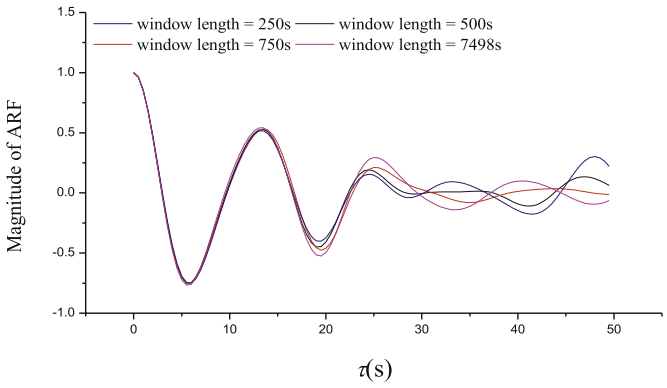

(b) ACF calculated from too small window lengths

Fig. 11. Ship motion Auto-correlation function.

Table 4
Memory length of impulse response function ($\varepsilon = 0.01$).

Impulse response functions IRF	Memory length τ (s)
h_{33}	14.4
h_{35}	12.2
h_{53}	12.2
h_{55}	13.9

shown in Fig. 12 and Table 5.

4.4. Predicted time series results by the IRF and ACF based optimization techniques

According to the calculation results in 4.3, we use the impulse response function and the Auto-correlation function to determine the input vector space of the Short-term prediction model for ship motion. In Table 4, the memory length of the impulse response function of the S175 container ship is 14.4s and 13.9s. And in Table 5, the correlation length of the Auto-correlation function of the S175 container ship is 20s, 16.5s, 15s and 13.9s. Since the sampling interval of the time series is 0.5, we can determine the input vector space of the model based on the memory time obtained by the two methods. In section 4.2 of the paper, we compared the calculation error of models with different input vector spaces, that is, parameter traversal methods, and obtained the best input vector space in each dataset. We can verify the accuracy of the obtained input vector space length by comparing them with the best value obtained by parameter traversal. The results are shown in Table 6. And based on the input vector space determined by the two methods, we also completed the training of the LSTM model and compared the prediction error. The result is shown in Fig. 13 and Table 7.

From the results in Tables 4–6, we find that two different input vector space determination methods can efficiently determine the input vector space of the model at a value close to the optimal threshold. But the performance of the model based on the determination method of the autocorrelation function tends to be better.

5. Conclusions

Deep learning neural networks are capable in processing nonlinear dynamic. The LSTM deep learning model provides a potential way for nonlinear ship motions prediction. It is critical to determine an optimal input vector dimension when training a LSTM model. Conventional method suffers both high computational cost and poor adaptation difficulties as it selects the optimal dimension by traversing an empirical preset range. The present work proposes an input vector space optimization method based on the dependence hidden in ship motion records of a sequence. Both the Impulse Response Function (IRF) based and Auto-correlation Function (ACF) based techniques are investigated for input vector space optimization. Numerical simulations are carried out for vilification and comparison. Concluding remarks are made as follows.

When keeping the other hyper parameters constant, prediction RMS

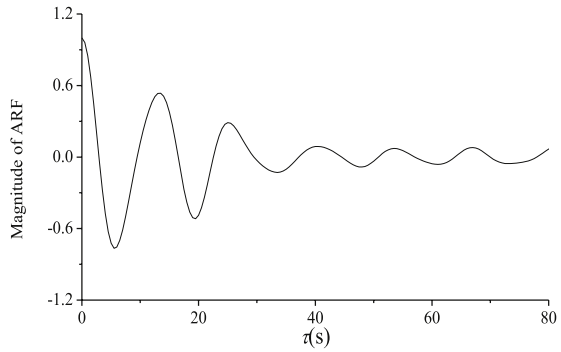

(a) Auto-correlation function for heave motion under the condition of sea state 5

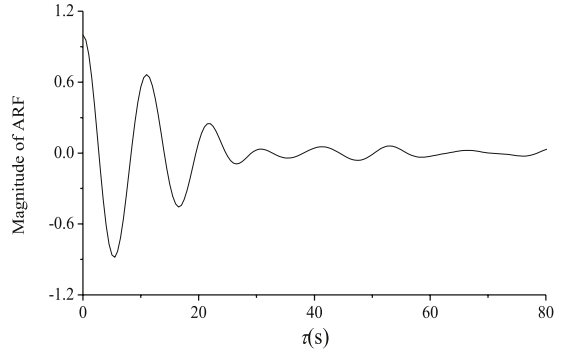

(b) Auto-correlation function for pitch motion under the condition of sea state 5

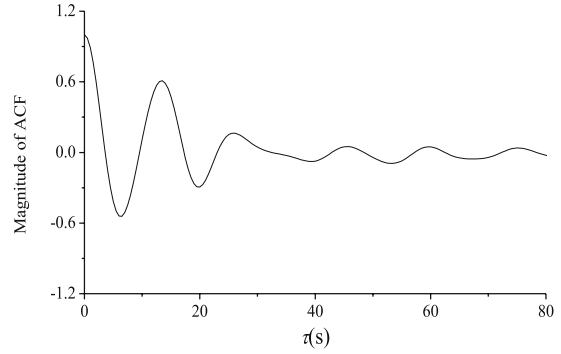

(c) Auto-correlation function for heave motion under the condition of sea state 6

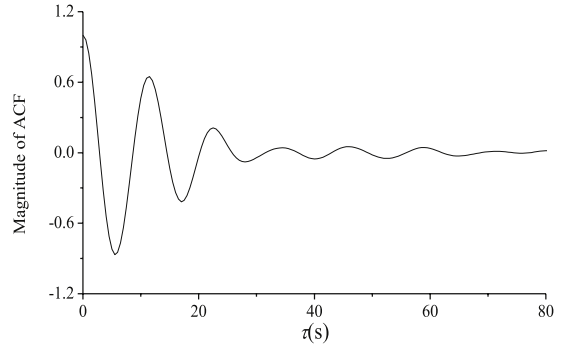

(d) Auto-correlation function for pitch motion under the condition of sea state 6

Fig. 12. ACF calculated from different window lengths.

Table 5
Correlation length of Auto-correlation function (r = 0.45).

Auto-correlation function (ACF)		Correlation length τ(s)
Sea state 5	Heave motion	20
	Pitch motion	16.5
Sea state 6	Heave motion	15
	Pitch motion	12.5

Table 6
Input vector space determined by two methods.

		Parameter traversal	Impulse response functions	Auto-correlation function
Sea state 5	Heave motion	40	29	40
	Pitch motion	35	28	33
Sea state 6	Heave motion	30	29	30
	Pitch motion	25	28	25

of the LSTM model increases and subsequently decreases as the input vector dimension grows. Simulation results under various sea condition consistently suggest that global optimum can be found in the prediction RMS functions. The optimal input vector dimension is obtained based on the global optimum where the prediction RMS is the least.

Compared to the conventional method, the proposed ship motion memory effects based input vector space optimization method provide a direct, effective and more efficient way. Both the IRF and the ACF techniques produce reasonable results which highly agree with the optimal input vector dimension. For example, the optimal input vector dimension with respect to the least prediction RMS is 35. The selected dimensions based on the IRF and the ACF techniques are 28 and 33, respectively.

In addition, comparison study is also carried out. It is found that the IRF and ACF techniques perform equivalently in training efficiency, while the ACF technique is better in prediction accuracy. As shown in Table 7, the prediction RMSs of the ACF-based LSTM model are smaller under various sea states. It results from that the memory effects of the nonlinear ship motions have nonlinearity while the IRFs are calculated based on linear hydrodynamic approach. The IRF technique is not capable in exactly representing the auto-correlations hidden in nonlinear ship motions. In contrast, the ACF technique is data-driven and without linear theoretical assumption. It calculates the auto-correlation measures by using the nonlinear ship motion time series. Hence, ACF technique can describe the nonlinear memory effects in ship motion more precisely and therefore performs better in input vector space optimization.

In summary, the proposed input vector space optimization method provides a feasible way to reduce computational cost and improve the adaptation when training a LSTM model.

CRediT authorship contribution statement

Yucheng Liu: Methodology, Software, Validation, Investigation, Writing - original draft. **Wenyang Duan:** Methodology, Supervision, Project administration, Funding acquisition. **Limin Huang:** Methodology, Conceptualization, Funding acquisition. **Shiliang Duan:** Methodology, Validation. **Xuewen Ma:** Methodology, Software.

Declaration of competing interest

The authors declare that they have no known competing financial interests or personal relationships that could have appeared to influence the work reported in this paper.

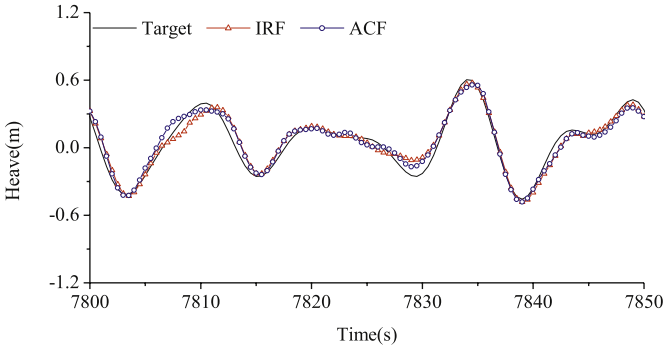

(a) Prediction results for heave motion under the condition of sea state 5

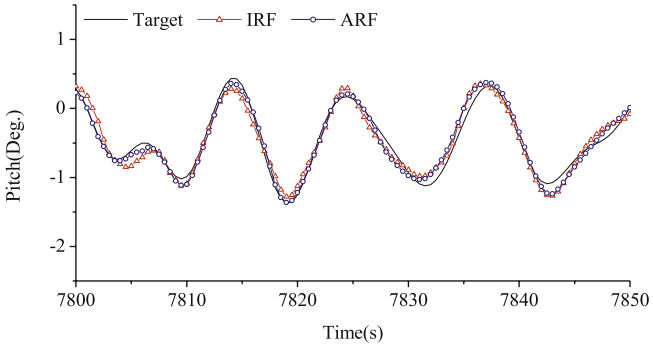

(b) Prediction results for pitch motion under the condition of sea state 5

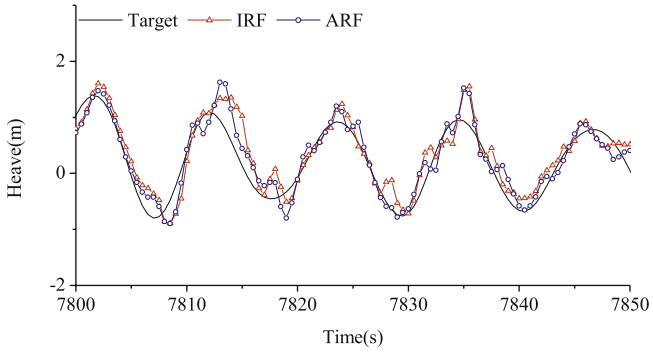

(c) Prediction results for heave motion under the condition of sea state 6

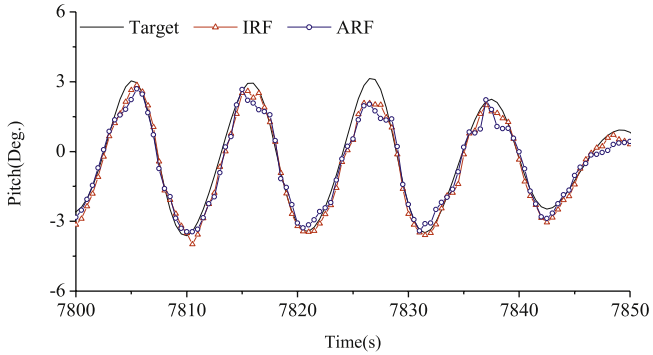

(d) Prediction results for pitch motion under the condition of sea state 6

Fig. 13. Prediction results of models with different input vector space determination methods.

Table 7
Prediction results of models with different input vector space determination methods.

	Sea state 5		Sea state 6	
	Heave motion RMSE(m)	Pitch motion RMSE (Deg.)	Heave motion RMSE(m)	Pitch motion RMSE (Deg.)
IRF	0.0770	0.1252	0.2794	0.4101
ACF	0.0742	0.1081	0.2736	0.3937

Acknowledgement

The present work is sponsored by the National Natural Science Foundation of China (Grant No. 51809066 and 51909039), State Key Laboratory of Ocean Engineering (Shanghai Jiao Tong University) (Grant No. 1902) and the Fundamental Research Funds for the Central Universities (Grants No. HEUCFJ170101, No. HEUCFP201707 and No. HEUCFM180107).

References

Akaike, H., 1974. A new look at the statistical model identification. In: In Selected Papers of Hirotugu Akaike. Springer, New York, NY, pp. 215–222.
Akaike, H., 1979. A Bayesian extension of the minimum AIC procedure of autoregressive model fitting. Biometrika 66 (2), 237–242.
Akita, R., Yoshihara, A., Matsubara, T., Uehara, K., 2016. Deep learning for stock prediction using numerical and textual information. In: In 2016 IEEE/ACIS 15th International Conference on Computer and Information Science (ICIS). IEEE, pp. 1–6.
Boden, M., 2002. A Guide to Recurrent Neural Networks and Backpropagation. The Dallas Project.
Chen, Y., Lv, Y., Li, Z., Wang, F., 2016. November). Long short-term memory model for traffic congestion prediction with online open data. In: In 2016 IEEE 19th International Conference on Intelligent Transportation Systems (ITSC). IEEE, pp. 132–137.
Cummins, W., 1962. The Impulse Response Function and Ship Motions (No. DTMB-1661). David Taylor Model Basin, Washington DC.
Duan, W., Huang, L., Han, Y., Wang, R., 2015. IRF-AR model for short-term prediction of ship motion. In: In the Twenty-Fifth International Ocean and Polar Engineering Conference. International Society of Offshore and Polar Engineers.
Duan, S., Ma, Q., Huang, L., Ma, X., 2019. July). A LSTM deep learning model for deterministic ship motions estimation using wave-excitation inputs. In: In the 29th International Ocean and Polar Engineering Conference. International Society of Offshore and Polar Engineers.
Gers, F., Schmidhuber, J., Cummins, F., 1999. Learning to Forget: Continual Prediction with LSTM.
Graves, A., Liwicki, M., Fernández, S., Bertolami, R., Bunke, H., Schmidhuber, J., 2008. A novel connectionist system for unconstrained handwriting recognition. IEEE Trans. Pattern Anal. Mach. Intell. 31 (5), 855–868.
Hochreiter, S., Schmidhuber, J., 1997. Long short-term memory. Neural Comput. 9 (8), 1735–1780.
Huang, L., Duan, W., Han, Y., Chen, Y., 2014. A review of short-term prediction techniques for ship motions in seaway. J. Ship Mech. 18 (12), 1534–1542.
Huang, L., Han, Y., Duan, W., Chen, Y., Ma, S., 2018. Numerical and experimental studies on a predictive control approach for pitch stabilization in heading waves. Ocean Eng. 169, 388–400.
Kaplan, P., 1965. A Preliminary Study of Prediction Techniques for Aircraft Carrier Motions at Sea (No. OCEANICS-65-23). OCEANICS INC PLAINVIEW NY.
Khan, A., Marion, K., Bil, C., 2007. The prediction of ship motions and attitudes using artificial neural networks. Asor Bulletin 26 (1), 2.
Kingma, D.P., Ba, J., 2014. Adam: A Method for Stochastic Optimization arXiv preprint arXiv:1412.6980.
Liapis, J., 1986. Time-domain Analysis of Ship Motions. University of Michigan.
Liu, H., Mi, X.W., Li, Y., 2018. Wind speed forecasting method based on deep learning strategy using empirical wavelet transform, long short term memory neural network and Elman neural network. Energy Convers. Manag. 156, 498–514.
Mak, B., Duz, B., 2019. June). Ship as A Wave buoy: estimating relative wave direction from in-service ship motion measurements using machine learning. In: In the 38th International Conference on Ocean, Offshore and Arctic Engineering.
Nielsen, U., Brodtkorb, A., Jensen, J., 2018. Response predictions using the observed autocorrelation function. Mar. Struct. 58, 31–52.
Shao, H., Soong, B., 2016. November). Traffic flow prediction with long short-term memory networks (LSTMs). In: In 2016 IEEE Region 10 Conference (TENCON). IEEE, pp. 2986–2989.
Triantafyllou, M., Athans, M., 1981. Real time estimation of the heaving and pitching motions of a ship, using a Kalman filter. In: In OCEANS, vol. 81. IEEE, pp. 1090–1095.
Triantafyllou, M., Athans, M., 1983. Real Time Estimation of Motions of a Destroyer Using Kalman Filtering Techniques. laboratory for information and Decision Systems Rep.
Triantafyllou, M.S., Bodson, M., 1982. Real Time Prediction of Marine Vessel Motions Using Kalman Filtering Techniques.
Wang, K., Li, G., 1997. DRNN neural network for time series prediction of ship rolling motion. J. Harbin Eng. Univ. 18, 39–44, 01.
Weng, Z., Gu, M., Liu, C., 2010. Extreme short-term prediction of ship motion based on second-order adaptive Volterra series. J. Ship Mech. 7.
Yang, X., 2013. Displacement motion prediction of a landing deck for recovery operations of rotary UAVs. Int. J. Contr. Autom. Syst. 11 (1), 58–64.
Yumori, I., 1981. Real time prediction of ship response to ocean waves using time series analysis. In: OCEANS, vol. 81. IEEE, pp. 1082–1089.
Zhao, B., Duan, W., Ertekin, R., Hayatdavoodi, M., 2015. High-level Green–Naghdi wave models for nonlinear wave transformation in three dimensions. J. Ocean Eng. Marine Eng. 1 (2), 121–132.
Zhao, Z., Chen, W., Wu, X., Chen, P., Liu, J., 2017. LSTM network: a deep learning approach for short-term traffic forecast. IET Intell. Transp. Syst. 11 (2), 68–75.